United States Department of Commerce
Technology Administration
National Institute of Standards and Technology

NISTIR 5007

DUAL-PORT CIRCULARLY POLARIZED PROBE STANDARDS AT THE NATIONAL INSTITUTE OF STANDARDS AND TECHNOLOGY

M.H. Francis
Katherine MacReynolds
Seturnino Canales

NISTIR 5007

DUAL-PORT CIRCULARLY POLARIZED PROBE STANDARDS AT THE NATIONAL INSTITUTE OF STANDARDS AND TECHNOLOGY

M.H. Francis
Katherine MacReynolds
Seturnino Canales

Electromagnetic Fields Division
Electronics and Electrical Engineering Laboratory
National Institute of Standards and Technology
Boulder, Colorado 80303-3328

August 1993

U.S. DEPARTMENT OF COMMERCE, Ronald H. Brown, Secretary
TECHNOLOGY ADMINISTRATION, Mary L. Good, Under Secretary for Technology
NATIONAL INSTITUTE OF STANDARDS AND TECHNOLOGY, Arati Prabhakar, Director

CONTENTS

Page

1. INTRODUCTION 1

2. NEED FOR CP STANDARDS 1

3. DESIGN REQUIREMENTS 3

4. MEASUREMENT TECHNIQUES 4

5. MEASUREMENT RESULTS 5

6. MEASUREMENT UNCERTAINTIES 14

7. SUMMARY 25

8. ACKNOWLEDGEMENTS 25

9. REFERENCES 25

Dual-Port Circularly Polarized Probe Standards at the National Institute of Standards and Technology

Michael H. Francis, Katherine MacReynolds, and Seturnino Canales

Electromagnetic Fields Division
National Institute of Standards and Technology
Boulder, Colorado 80303-3328

The National Institute of Standards and Technology has acquired dual-port circularly polarized probes to use as gain and near-field probe standards for measuring circularly polarized test antennas. These probes will serve as standards for the 18 to 26.5, 33 to 50, and 50 to 70 GHz frequency bands. This paper discusses the need for such standards, their design requirements, the measurement results for gain, polarization, and pattern, and an uncertainty analysis of the measurements.

Key words: antenna measurements; circularly polarized probe; near-field probe; polarization

1. INTRODUCTION

Scientists at the National Institute of Standards and Technology (NIST) recognized several years ago that we needed to have circularly polarized (cp) probes to serve as gain and near-field probe standards for the measurement of cp antennas (for example, the Milstar program). Beginning in 1990, NIST began acquiring and calibrating dual-port cp probes to use as cp standards operating in the 18 to 26.5 GHz, 33 to 50 GHz, and 50 to 75 GHz frequency bands.

Section 2 discusses the need for cp standards. Section 3 considers the design requirements for these cp standards. Section 4 examines the techniques used to measure these cp standards. Section 5 reports the measurement results, and section 6 analyzes the measurement uncertainties. Finally, Section 7 contains a summary.

2. NEED FOR CP STANDARDS

Many test antennas are measured using the near-field technique. This technique requires correction for the effects of the probes. The probe correction is generally more accurate if the probes have the same type of polarization as the antenna under test (AUT).

That is, the correction is better if we measure a cp AUT with cp probes and a linearly polarized AUT with linearly polarized probes.

Let us consider the probe correction equations. The main- and cross-component far-field spectra of an AUT are given by [1]

$$t_m = \frac{\frac{D'}{s_m'} - \frac{D''}{s_c''}\rho_s'}{1 - \frac{\rho_s'}{\rho_s''}} \tag{1}$$

for the main component, and

$$t_c = \frac{\frac{D''}{s_c''} - \frac{D'}{s_m'\rho_s''}}{1 - \frac{\rho_s'}{\rho_s''}} \tag{2}$$

for the cross component. In eq (1) and (2) D' is the coupling product of the AUT and probe 1 and D'' is the coupling product of the AUT with probe 2. s_m' is the spectra of the component of probe 1 that is nominally copolarized to the AUT, and s_c'' is the spectra of the component of probe 2 that is nominally cross polarized to the AUT. ρ_s' is the polarization ratio (s_c'/s_m') of the nominally copolarized probe, and ρ_s'' is the polarization ratio (s_c''/s_m'') of the cross-polarized probe. All of these quantities are functions of the wave vector $\bar{k}$.

If $|s_c'| << |s_m'|$, then the second term in eq (1) is negligible since $|\rho_s'| << 1$. Similarly, if $|s_c''| >> |s_m''|$, then the second term in eq (2) is negligible since $|1/\rho_s''| << 1$. This is often the case with polarization-matched antennas. For example, if the AUT is Y-polarized, probe 1 is Y-polarized, and probe 2 is X-polarized. However, if the AUT is left cp, probe 1 is Y-polarized, and probe 2 is X-polarized, then these terms cannot be neglected. For this case the magnitudes of s_c' and s_m' are about the same, and the magnitudes of s_c'' and s_m'' are also about the same. Thus, the second terms in eq (1) and (2) cannot be neglected. This has important consequences for the numerical stability of eq

(2). For most directions $|t_c| << |t_m|$. Consequently, eq (2) is the small difference between large quantities, which is numerically unstable. We conclude that it is generally better to measure a cp AUT with cp probes than with linearly polarized probes. (Similarly, it is better to measure a linearly polarized AUT with linearly polarized probes than with cp probes.) Also, if we measure a cp test antenna with linearly polarized probes, we must measure both linearly polarized components to accurately determine the gain of a cp AUT. If the AUT has a good circular polarization and we measure the gain with a probe that has a good circular polarization, then the cross-component contribution to the gain is negligible.

3. DESIGN REQUIREMENTS

One requirement is that the cp probes be dual port. Equations (1) and (2) imply that we also need to know the relative phase between s_m' and s_c''. For a linearly polarized probe, this is easy to achieve since we can just rotate the probe by 90° to change a Y-polarized probe into an X-polarized (or an X-polarized probe to a Y-polarized probe). However, rotating a cp probe does not change its sense of polarization. If we have two physically separate probes they must be mounted separately. It is then difficult to accurately measure the phase between the probes since a separate alignment is necessary. Accurate alignments typically take 1-2 days per alignment so the system will probably drift considerably during the alignment period due to environmental changes such as temperature. However, a dual-port cp probe requires only one alignment, allowing more accurate phase measurements between probe 1 and probe 2.

Gruner [2] has shown that better polarization properties can be obtained with dual-port cp probes using an orthomode transducer (OMT) than with single-port cp probes. This is because some of the energy is reflected at the probe aperture, changes the sense of polarization, and returns back through the probe. If the orthogonal port of the OMT is properly matched and terminated, this cross-polarized reflected energy will be absorbed and will not be reradiated out the aperture as cross-polarized energy.

Since NIST performs probe gain and polarization measurements using a three-antenna method [3], it is necessary to have probes in sets of three. Some spread in gains is desirable to reduce the effects of multiple reflections between the probes [4], but not too much different. Otherwise, the insertion loss, when the antennas are inserted into the system, will be large and difficult to measure accurately.

Finally, to prevent the polarization properties of one port from being affected by the load on the other port, it is necessary to have good isolation between the ports and a good return loss at the input of both ports.

To meet these conditions, these dual-port cp probes need to meet the requirements of table 1. In table 1, G_0 refers to the gain of the middle-sized probe in a set of three probes.

Table 1. Dual-port probe requirements.

Ports	Dual-port, 1 right cp, 1 left cp
Axial ratio	< 1.0 dB
Port-to-port isolation	> 25 dB
Return loss at input ports	> 20 dB
Gains	G_0 - 5 dB, G_0, G_0 + 5 dB

NIST had 18 dual-port cp probes built to serve as standards in the WR42 (18 to 26.5 GHz), WR22 (33 to 50 GHz), and WR15 (50 to 75 GHz) waveguide bands. Two sets of probes were necessary to cover each band and still meet the axial ratio requirements. Figure 1 shows an assembly drawing of one of these dual-port probes. The other probes have similar designs.

4. MEASUREMENT TECHNIQUES

The gains were measured using the three-antenna technique described in detail by ref. [3]. Briefly, we determine the gain by (1) measuring the received output power as a function of the separation distance z between two of the probes, (2) doing a least-squares fit in powers of (1/z) where the leading term is proportional to the square root of the product of the probe gains, and (3) using the results from each of the three unique pair combinations to solve for the individual probe gains.

We determine the polarizations using the technique described by Newell et al. [5]. For this method, we need to measure the on-axis amplitude and phase difference between the two ports of each dual-port probe. Then, with the two probes hooked to the ports with the same sense of polarization (for example, both on the left circularly polarized port) and looking directly at each other, we set the amplitude to 0 dB and the phase to 0°. Next, we put the receiving probe on the cross-polarized port and rotate the receiving probe about an axis that is perpendicular to the probe aperture. After doing the same for the other cross-polarized port combination, we use the resulting curves to obtain the on-axis axial ratios and tilt angles for both ports of both probes. Since we have three pair combinations, we obtain the axial ratio and tilt angle of each port of each probe twice. (We could also obtain the

axial ratio and tilt angle of each port of each probe by rotating a linearly polarized probe against each of the cp probes.)

We measure the probe patterns using the technique described by ref. [6]. This measurement is performed in the far field. One of the dual-port probes is used as the source antenna and the probe under test as the receiving antenna. The source antenna does not rotate or move after it is aligned, so we need to know only its on-axis axial ratio and tilt angle to correct the measured pattern for the source. We rotate the receiving probe about two axes as indicated in figure 2. The first axis is the z axis which is perpendicular to the receiving-probe aperture and the second axis is the vertical axis which intersects with the z-axis and lies in the plane of the probe aperture. In this way, we can scan through an entire sphere of data or, more commonly, just the forward hemisphere. (Only the forward hemisphere is important if we use the probe as a standard for a planar near-field measurement.)

5. MEASUREMENT RESULTS

To cover the frequency ranges of interest (18 to 26.5, 33 to 50, and 50 to 75 GHz), we required 6 sets of dual-port cp probes (that is, 18 probes in all). We measured the gain and polarization of each probe at 3 frequencies over its operating band. Tables 2-7 show the gain and polarization results for the WR42 (18 to 26.5 GHz) probes, tables 8-13 show the results for the WR22 (33 to 50 GHz) probes, and tables 14-19 show the results for the WR15 (50 to 75 GHz) probes. We indicate those probes in the lower portion of each waveguide band by adding the suffix 'A' to the waveguide band designation (for example, WR42A). The suffix 'B' indicates those probes in the upper portion of each waveguide band. Within each portion of a waveguide band, the tables list the probes in ascending order of the gain.

Table 2. Gain and polarization for WR42A probe SN118.

Frequency (GHz)	Port	Gain (dB)	Axial ratio (dB)	Tilt angle (deg)
20.2	Right	11.07 ± 0.11	0.04 ± 0.05	-21 ± 45
	Left	11.00 ± 0.11	0.04 ± 0.05	59 ± 45
20.7	Right	11.27 ± 0.11	0.06 ± 0.05	-53 ± 24
	Left	11.24 ± 0.11	0.04 ± 0.05	-4 ± 45
21.2	Right	11.65 ± 0.11	0.03 ± 0.05	-70 ± 45
	Left	11.69 ± 0.11	0.07 ± 0.05	14 ± 24

Table 3. Gain and polarization for WR42A probe SN 119.

Frequency (GHz)	Port	Gain (dB)	Axial ratio (dB)	Tilt angle (deg)
20.2	Right	17.44 ± 0.11	0.13 ± 0.03	0 ± 9
	Left	17.44 ± 0.11	0.13 ± 0.03	-89 ± 9
20.7	Right	17.64 ± 0.11	0.04 ± 0.05	34 ± 45
	Left	17.60 ± 0.11	0.04 ± 0.05	-53 ± 45
21.2	Right	18.20 ± 0.11	0.05 ± 0.05	14 ± 24
	Left	18.11 ± 0.11	0.05 ± 0.05	-85 ± 45

Table 4. Gain and polarization for WR42A probe SN 120.

Frequency (GHz)	Port	Gain (dB)	Axial ratio (dB)	Tilt angle (deg)
20.2	Right	23.36 ± 0.11	0.04 ± 0.05	48 ± 45
	Left	23.35 ± 0.11	0.02 ± 0.05	-47 ± 45
20.7	Right	23.87 ± 0.11	0.08 ± 0.05	84 ± 24
	Left	23.88 ± 0.11	0.08 ± 0.05	-12 ± 24
21.2	Right	24.36 ± 0.11	0.10 ± 0.03	85 ± 9
	Left	24.44 ± 0.11	0.10 ± 0.04	2 ± 10

Table 5. Gain and polarization for WR42B probe SN 02.

Frequency (GHz)	Port	Gain (dB)	Axial ratio (dB)	Tilt angle (deg)
21.8	Right	11.96 ± 0.11	0.40 ± 0.03	-85 ± 9
	Left	11.96 ± 0.11	0.37 ± 0.03	6 ± 9
24.3	Right	13.28 ± 0.11	0.19 ± 0.03	-10 ± 9
	Left	13.21 ± 0.11	0.20 ± 0.03	80 ± 9
26.5	Right	13.40 ± 0.11	0.16 ± 0.03	-80 ± 9
	Left	13.49 ± 0.11	0.09 ± 0.05	41 ± 24

Table 6. Gain and polarization for WR42B probe SN 01.

Frequency (GHz)	Port	Gain (dB)	Axial ratio (dB)	Tilt angle (deg)
21.8	Right	18.78 ± 0.11	0.41 ± 0.03	86 ± 9
	Left	18.82 ± 0.11	0.47 ± 0.03	-2 ± 9
24.3	Right	19.29 ± 0.11	0.12 ± 0.03	4 ± 9
	Left	19.21 ± 0.11	0.12 ± 0.03	-85 ± 9
26.5	Right	19.40 ± 0.11	0.21 ± 0.03	87 ± 9
	Left	19.53 ± 0.11	0.19 ± 0.03	-4 ± 9

Table 7. Gain and polarization for WR42B probe SN 03.

Frequency (GHz)	Port	Gain (dB)	Axial ratio (dB)	Tilt angle (deg)
24.3	Right	25.66 ± 0.11	0.62 ± 0.03	-81 ± 9
	Left	25.66 ± 0.11	0.58 ± 0.03	7 ± 9
24.3	Right	26.20 ± 0.11	0.09 ± 0.05	-22 ± 9
	Left	26.20 ± 0.11	0.14 ± 0.03	78 ± 9
26.5	Right	26.75 ± 0.11	0.24 ± 0.03	-79 ± 9
	Left	26.77 ± 0.11	0.13 ± 0.05	- 2 ± 24

Table 8. Gain and polarization for WR22A probe SN 03.

Frequency (GHz)	Port	Gain (dB)	Axial ratio (dB)	Tilt angle (deg)
33	Right	15.72 ± 0.15	0.35 ± 0.05	- 1 ± 13
	Left	15.50 ± 0.15	0.32 ± 0.05	-87 ± 13
36.5	Right	15.93 ± 0.15	0.09 ± 0.08	86 ± 25
	Left	15.42 ± 0.15	0.13 ± 0.05	- 1 ± 13
40	Right	15.16 ± 0.15	0.24 ± 0.05	13 ± 13
	Left	15.49 ± 0.15	0.32 ± 0.05	-86 ± 13

Table 9. Gain and polarization for WR22A probe SN 01.

Frequency (GHz)	Port	Gain (dB)	Axial ratio (dB)	Tilt angle (deg)
33	Right	21.05 ± 0.15	0.43 ± 0.05	14 ± 13
	Left	20.94 ± 0.15	0.43 ± 0.05	-86 ± 13
36.5	Right	21.97 ± 0.15	0.25 ± 0.05	56 ± 13
	Left	21.46 ± 0.15	0.16 ± 0.05	3 ± 13
40	Right	21.87 ± 0.15	0.30 ± 0.05	33 ± 13
	Left	21.91 ± 0.15	0.23 ± 0.05	-84 ± 13

Table 10. Gain and polarization for WR22A probe SN 02.

Frequency (GHz)	Port	Gain (dB)	Axial ratio (dB)	Tilt angle (deg)
33	Right	20.94 ± 0.15	0.50 ± 0.05	- 2 ± 13
	Left	25.78 ± 0.15	0.47 ± 0.05	88 ± 13
36.5	Right	26.75 ± 0.15	0.14 ± 0.05	84 ± 13
	Left	26.55 ± 0.15	0.15 ± 0.05	5 ± 13
40	Right	26.21 ± 0.15	0.16 ± 0.05	31 ± 13
	Left	27.00 ± 0.15	0.20 ± 0.05	-88 ± 13

Table 11. Gain and polarization for WR22B probe SN121.

Frequency (GHz)	Port	Gain (dB)	Axial ratio (dB)	Tilt angle (deg)
44.5	Right	17.39 ± 0.15	0.121 ± 0.05	-24 ± 21
	Left	17.20 ± 0.15	0.218 ± 0.05	50 ± 18
44.5	Right	17.74 ± 0.15	0.103 ± 0.05	-21 ± 21
	Left	17.57 ± 0.15	0.160 ± 0.05	53 ± 21
45.5	Right	17.93 ± 0.15	0.189 ± 0.05	-20 ± 21
	Left	17.82 ± 0.15	0.245 ± 0.05	59 ± 18

Table 12. Gain and polarization for WR22B probe SN 122.

Frequency (GHz)	Port	Gain (dB)	Axial ratio (dB)	Tilt angle (deg)
43.5	Right	24.00 ± 0.15	0.086 ± 0.05	43 ± 24
	Left	23.78 ± 0.15	0.112 ± 0.05	-45 ± 21
44.5	Right	24.30 ± 0.15	0.082 ± 0.05	49 ± 24
	Left	24.32 ± 0.15	0.141 ± 0.05	-50 ± 21
45.5	Right	24.68 ± 0.15	0.107 ± 0.05	14 ± 21
	Left	24.70 ± 0.15	0.156 ± 0.05	-68 ± 21

Table 13. Gain and polarization for WR22B probe SN 123.

Frequency (GHz)	Port	Gain (dB)	Axial ratio (dB)	Tilt angle (deg)
43.5	Right	28.03 ± 0.15	0.133 ± 0.05	61 ± 21
	Left	27.88 ± 0.15	0.173 ± 0.05	-47 ± 21
44.5	Right	28.16 ± 0.15	0.175 ± 0.05	75 ± 21
	Left	28.00 ± 0.15	0.204 ± 0.05	-15 ± 18
45.5	Right	28.24 ± 0.15	0.125 ± 0.05	78 ± 21
	Left	28.17 ± 0.15	0.161 ± 0.05	-37 ± 21

Table 14. Gain and polarization for WR15A probe SN 303.

Frequency (GHz)	Port	Gain (dB)	Axial ratio (dB)	Tilt angle (deg)
50	Right	10.22 ± 0.19	0.29 ± 0.13	22 ± 21
	Left	9.82 ± 0.19	0.29 ± 0.13	-79 ± 21
55	Right	10.91 ± 0.19	0.18 ± 0.13	57 ± 21
	Left	10.49 ± 0.19	0.10 ± 0.13	60 ± 40
60	Right	12.04 ± 0.19	0.57 ± 0.13	2 ± 21
	Left	11.89 ± 0.19	0.63 ± 0.13	76 ± 21

Table 15. Gain and polarization for WR15A probe SN 302.

Frequency (GHz)	Port	Gain (dB)	Axial ratio (dB)	Tilt angle (deg)
50	Right	17.88 ± 0.19	0.20 ± 0.13	44 ± 21
	Left	16.79 ± 0.19	0.10 ± 0.13	89 ± 40
55	Right	18.15 ± 0.19	0.20 ± 0.13	61 ± 21
	Left	17.45 ± 0.19	0.18 ± 0.13	0 ± 21
60	Right	17.94 ± 0.19	0.44 ± 0.13	9 ± 21
	Left	17.44 ± 0.19	0.27 ± 0.13	-88 ± 21

Table 16. Gain and polarization for WR15A probe SN 304.

Frequency (GHz)	Port	Gain (dB)	Axial ratio (dB)	Tilt angle (deg)
50	Right	23.87 ± 0.19	0.29 ± 0.13	-10 ± 21
	Left	23.26 ± 0.19	0.32 ± 0.13	82 ± 21
55	Right	24.69 ± 0.19	0.11 ± 0.13	-71 ± 40
	Left	23.99 ± 0.19	0.10 ± 0.13	20 ± 40
60	Right	24.71 ± 0.19	0.28 ± 0.13	-16 ± 21
	Left	24.19 ± 0.19	0.32 ± 0.13	-90 ± 21

Table 17. Gain and polarization for WR15B probe SN 011.

Frequency (GHz)	Port	Gain (dB)	Axial ratio (dB)	Tilt angle (deg)
60	Right	11.64 ± 0.19	0.50 ± 0.13	0 ± 21
	Left	11.39 ± 0.19	0.53 ± 0.13	78 ± 21
65	Right	12.65 ± 0.19	0.18 ± 0.13	77 ± 21
	Left	12.27 ± 0.19	0.23 ± 0.13	18 ± 21
71	Right	12.49 ± 0.19	1.00 ± 0.45	72 ± 29
	Left	12.80 ± 0.19	0.80 ± 0.45	90 ± 29

Table 18. Gain and polarization for WR15B probe SN 012.

Frequency (GHz)	Port	Gain (dB)	Axial ratio (dB)	Tilt angle (deg)
60	Right	19.10 ± 0.19	0.45 ± 0.13	0 ± 21
	Left	19.13 ± 0.19	0.37 ± 0.13	90 ± 21
65	Right	19.77 ± 0.19	0.28 ± 0.13	72 ± 21
	Left	19.56 ± 0.19	0.23 ± 0.13	18 ± 21
71	Right	20.61 ± 0.19	0.35 ± 0.45	72 ± 29
	Left	19.85 ± 0.19	0.30 ± 0.45	0 ± 29

Table 19. Gain and polarization for WR15B probe SN 013.

Frequency (GHz)	Port	Gain (dB)	Axial ratio (dB)	Tilt angle (deg)
60	Right	25.49 ± 0.19	0.28 ± 0.13	-12 ± 21
	Left	25.52 ± 0.19	0.38 ± 0.13	72 ± 21
65	Right	26.38 ± 0.19	0.38 ± 0.13	-72 ± 21
	Left	26.10 ± 0.19	0.28 ± 0.13	27 ± 21
71	Right	26.08 ± 0.19	0.23 ± 0.45	72 ± 29
	Left	26.18 ± 0.19	0.30 ± 0.45	36 ± 29

The probes in WR42A and WR22B waveguide bands were calibrated at three closely spaced frequencies as compared to the probes in the other waveguide bands. We did this so that we could use these as standards at the specific frequencies of interest for one of our customers.

We also used an automated network analyzer (ANA) to measure the return loss of each port of each probe and to measure the port-to-port isolation of each probe. All return losses were 20 dB or greater and all port-to-port isolations were greater than 25 dB. Figures 3 and 4 show some sample ANA results.

Figures 5-8 show sample contour plots of the main- and cross-component patterns for amplitude and phase. Since probe correction is done in k-space, these contours are shown as a function of k_x/k and k_y/k, where $k=2\pi/\lambda$, and k_x/k = cos(elevation) sin(azimuth), and k_y/k = sin(elevation). Each cross component has two nulls in the pattern. These nulls correspond to the two points where the cross component of the horn is equal in amplitude and 180° out of phase with the cross component of the polarizer. Thus, the probe's cross polarization is a minimum at these points.

6. MEASUREMENT UNCERTAINTIES

Repjar et al. [3] describe the techniques that NIST uses to determine the uncertainties in the measurement of gain and polarization. Tables 20-22 show the uncertainties in gain for each waveguide band.

Table 20. Probe gain uncertainties for WR42 measurements.

Source of uncertainty	Uncertainty (dB)
Systematic	
System drift & receiver nonlinearity	0.05
Attenuator calibration	0.05
Impedance mismatch	< 0.01
Distance nonlinearity	0.02
Residual multipath	0.03
Antenna alignment	0.05
Numerical fit uncertainty	0.03
Random	
Noise	0.02
Repeatability	0.02
RSS Uncertainty	0.11

Table 21. Probe gain uncertainties for WR22 measurements.

Source of uncertainty	Uncertainty (dB)
Systematic	
System drift & receiver nonlinearity	0.05
Attenuator calibration	0.10
Impedance mismatch	0.03
Distance nonlinearity	0.02
Residual multipath	0.02
Antenna alignment	0.05
Numerical fit uncertainty	0.03
Random	
Noise	0.02
Repeatability	0.07
RSS Uncertainty	0.15

Table 22. Probe gain uncertainty estimate for WR15 measurements.

Source of uncertainty	Uncertainty (dB)
Systematic	
System drift & receiver nonlinearity	0.15
Attenuator calibration	0.15
Impedance mismatch	0.03
Distance nonlinearity	0.02
Residual multipath	0.02
Antenna alignment	0.05
Numerical fit uncertainty	0.03
Random	
Noise	0.05
Repeatability	0.07
RSS Uncertainty	0.20

System drift, receiver nonlinearity, attenuator calibration, and antenna alignment are major sources of uncertainty for all waveguide bands. The uncertainty in the attenuator calibration increases with increasing frequency largely because of the reduced signal-to-noise ratio and because of poorer rf connections at higher frequencies.

In the WR42 waveguide band measurement repeatability is not a problem. However in the WR22 and WR15 waveguide bands repeatability is a major source of uncertainty. At these frequencies waveguide flanges have raised center bosses which make connections difficult to repeat with the same precision as at lower frequencies.

Noise is also a significant source of uncertainty in the WR15 band. This is because the waveguide attenuation increases with increasing frequency and is about 1.5 dB/m in this band, so the received signal decreases relative to the noise.

Tables 23-28 contain the uncertainty budgets for the polarization parameters.

Table 23. Axial ratio uncertainty estimate for WR42 measurements.

Source of uncertainty	Uncertainty in dB for AR ≥ 0.1 dB	Uncertainty in dB for 0.05 dB ≤ AR < 0.1 dB	Uncertainty in dB for AR ≤ 0.05 dB
Systematic			
Alignment	0.02	0.04	0.03
Multipath	0.02	0.02	0.03
Random			
Noise	< 0.01	< 0.01	0.01
Repeatability	0.01	0.01	0.01
RSS Uncertainty	0.03	0.05	0.05

Table 24. Tilt angle uncertainty estimate for WR42 measurements.

Source of uncertainty	Uncertainty in deg for AR ≥ 0.1 dB	Uncertainty in deg for 0.05 dB ≤ AR < 0.1 dB	Uncertainty in deg for AR ≤ 0.05 dB
Systematic			
Alignment	5	20	33
Multipath	7	13	25
Random			
Noise	< 1	1	7
Repeatability	1	2	16
RSS Uncertainty	9	24	45

Table 25. Axial ratio uncertainty estimate for WR22 measurements.

Source of uncertainty	Uncertainty in dB for AR ≥ 0.2 dB	Uncertainty in dB for 0.1 dB ≤ AR < 0.2 dB	Uncertainty in dB for 0.05 dB ≤ AR < 0.1 dB
Systematic			
Alignment	0.01	0.04	0.04
Multipath	0.02	0.02	0.02
Random			
Noise	< 0.01	< 0.01	0.01
Repeatability	0.01	0.01	0.01
RSS Uncertainty	0.05	0.05	0.05

Table 26. Tilt angle uncertainty estimate for WR22 measurements.

Source of uncertainty	Uncertainty in deg for AR ≥ 0.2 dB	Uncertainty in deg for 0.1 dB ≤ AR < 0.2 dB	Uncertainty in deg for 0.05 dB ≤ AR < 0.1 dB
Systematic			
Alignment	18	20	20
Multipath	3	7	13
Random			
Noise	2	2	2
Repeatability	1	1	1
RSS Uncertainty	18	21	24

Table 27. Axial ratio uncertainty estimate for WR15 measurements.

Source of uncertainty	Uncertainty in dB for AR ≤ 0.15 dB	Uncertainty in dB for AR ≥ 0.15 dB
Systematic		
Alignment	0.05	0.1
Multipath	0.01	0.01
Random		
Noise	0.07	0.07
Repeatability	0.06	0.06
RSS Uncertainty	0.11	0.13

Table 28. Tilt angle uncertainty estimate for WR15 measurements.

Source of uncertainty	Uncertainty in deg for AR ≤ 0.15 dB	Uncertainty in deg for AR ≥ 0.15 dB
Systematic		
Alignment	31	12
Multipath	10	5
Random		
Noise	20	15
Repeatability	10	5
RSS Uncertainty	40	21

The alignment uncertainty is a major source of uncertainty at all frequencies. This uncertainty increases as the frequency increases. This is a result of the decreasing physical size of the probes with increasing frequency. A physically small object is harder to align with a transit. This was especially a problem for the lower gain horns in the WR15 band, which were only about 1 cm in diameter. Noise also becomes an increasing problem as the frequency increases for the same reasons we discussed above in regard to the gain uncertainty. The uncertainty due to noise was greater at 71 GHz due to a decrease in system power output. Thus, the uncertainty in axial ratio for this frequency is 0.45 dB and the uncertainty in tilt angle is 29°. The uncertainty in the polarization parameters also increases with decreasing axial ratio. This is because as the axial ratio decreases the polarization ellipse approaches a circle and the tilt angle becomes poorly defined.

Tables 29-31 contain the probe pattern uncertainties as a function of relative amplitude below the peak.

The major sources of uncertainty in the probe pattern amplitude are multiple reflections between the source and receiving antennas, antenna alignment, and the limited dynamic range of the receive system. Drift, near-zone effects, and uncertainty in the port-to-port phase are the major sources of uncertainty in the phase. Drift was a significant problem in the WR15 frequency band. For this frequency band, accurate phase measurements are impossible without the use of tie scans to correct the phase for temperature variation. (Tie scans are a series of five scans taken in the ϕ direction. The middle scan of the five goes through the peak. This scanning in the ϕ direction contrasts with the normal scanning in the θ direction for the full two-dimensional data. Because tie scans require a much shorter time to take they can be used to correct for amplitude and phase drift.) A complete measurement scan takes about 4 h. We found that at WR15 frequencies a 0.1 °C change in temperature caused a change in phase of about 10°. By using tie scans we were able to limit the uncertainty in phase to 5-10° even though the temperature varied as much as 1-2 °C during a measurement.

Table 29. Probe pattern uncertainties for WR42 measurements.

Source of uncertainty	Amplitude uncertainty (dB) for levels of (relative to mainbeam)				Phase uncertainty (deg) for levels of (relative to mainbeam)			
	-5 dB	-15 dB	-30 dB	-45 dB	-5 dB	-45 dB	-30 dB	-45 dB
Systematic								
Multiple rfl.	0.02	0.05	0.3	1.5	0.2	0.1	2.	11.
Alignment	0.25	0.35	0.35	2.0	0.1	0.1	0.1	7.
Rcv. nonlin.	0.01	0.02	0.05	0.1	<0.1	0.1	0.3	1.
NZ effects	0.10	0.10	0.1	0.1	6.	6.	6.	6.
Rotator err.	0.01	0.02	0.02	0.1	<0.1	<0.1	<0.1	0.4
Dynamic range	0.01	0.03	0.15	0.8	<0.1	0.2	1.	6.
Drift	0.05	0.05	0.1	0.2	2.	2.	5.	10.
Port-to-port	0.10	0.10	0.2	0.2	5.	5.	10.	10.
Random								
Noise	<0.01	<0.01	<0.01	0.02	<0.1	<0.1	<0.1	0.1
RSS uncertainty	0.30	0.40	0.6	3.1	8.	8.	13.	21.

Table 30. Probe pattern uncertainties for WR22 measurements.

Source of uncertainty	Amplitude uncertainty (dB) for levels of (relative to mainbeam)				Phase uncertainty (deg) for levels of (relative to mainbeam)			
	-5 dB	-15 dB	-30 dB	-45 dB	-5 dB	-45 dB	-30 dB	-45 dB
Systematic								
Multiple rfl.	0.01	0.1	0.6	5.	0.3	0.7	4.	22.
Alignment	0.25	0.25	0.25	2.5	3.	3.	3.	10.
Rcv. nonlin.	0.01	0.02	0.05	0.1	<0.1	0.1	0.3	1.
NZ effects	0.10	0.1	0.1	0.1	6.	6.	6.	6.
Rotator err.	0.01	0.01	0.01	0.14	0.2	0.2	0.2	0.6
Dynamic range	0.01	0.03	0.15	0.8	<0.1	0.2	1.	6.
Drift	0.10	0.1	0.1	0.2	5.	5.	5.	5.
Port-to-port	0.10	0.1	0.2	0.2	5.	5.	10.	10.
Random								
Noise	<0.01	<0.01	<0.01	0.02	<0.1	<0.1	<0.1	0.1
RSS uncertainty	0.32	0.33	0.8	5.	10.	10.	14	28.

Table 31. Probe pattern uncertainties for WR15 measurements.

Source of uncertainty	Amplitude uncertainty (dB) for levels of (relative to mainbeam)				Phase uncertainty (deg) for levels of (relative to mainbeam)			
	-5 dB	-15 dB	-30 dB	-45 dB	-5 dB	-15 dB	-30 dB	-45 dB
Systematic								
Multiple rfl.	0.01	0.1	0.4	3.	0.3	0.7	4.	22.
Alignment	0.25	0.4	0.4	0.6	3.	3.	3.	10.
Rcv. nonlin.	0.1	0.1	0.2	0.3	0.7	0.7	1.3	2.
NZ effects	0.2	0.2	0.2	0.2	12.	12.	12.	12.
Rotator err.	0.01	0.02	0.02	0.03	<0.1	<0.1	<0.1	<0.1
Dynamic range	0.05	0.15	0.8	4.	0.3	1.	6.	29.
Drift	0.1	0.1	0.2	0.2	10.	10.	10.	10.
Port-to-port	0.3	0.3	0.3	0.3	15.	15.	15.	15.
Random								
Noise	<0.01	<0.01	<0.01	0.02	<0.1	<0.1	<0.1	0.1
RSS uncertainty	0.5	0.6	1.3	7.	22.	22.	23.	44.

7. SUMMARY

We have acquired and calibrated dual-port cp probes to serve as standards for cp antenna measurements. These standards cover the WR42 (18 to 26.5 GHz), WR22 (33 to 50 GHz), and WR15 (50 to 75 GHz) frequency bands. Thus, NIST is now able to offer measurement services for the gain, polarization, and pattern of cp antennas in these frequency bands.

8. ACKNOWLEDGEMENTS

We thank Doug Tamura for performing many of the measurements, Jeff Guerrieri for processing some of the data, and Doug Kremer for designing the probe mounts. We thank Bob Gruner of Comsat Laboratories for designing and building the probes. We also thank the Coordination Calibration Group of the Department of Defense for funding this effort.

9. REFERENCES

[1] Newell, A.C., "Error analysis techniques for planar near-field measurements," IEEE Trans. Antenna Propagat. AP-36, pp 754-768, June 1988.

[2] Gruner, R.W., "Design procedure for a distributed reactance polarizer," IEEE AP-S International Symposium Proceedings, Vancouver, British Columbia, pp. 635-638, June 1985.

[3] Repjar, A.G.; Newell, A.C.; Tamura, D.T., "Extrapolation range measurements for determining antenna gain and polarization," Natl. Bur. Stand. (U.S.) Tech. Note 1311, August 1987.

[4] Francis, M.H. and MacReynolds, K., "Evaluation of dual-port circularly polarized probes for planar near-field measurements," Proceedings of the Antenna Measurement Techniques Association, vol. 12, pp. 13-3 to 13-8, October 1990.

[5] Newell, A.C.; Kremer, D.P.; Guerrieri, J.R., "Improvements in polarization measurements of circularly polarized antennas," Proceedings of the Antenna Measurement Techniques Association, vol. 11, pp. 1-30 to 1-35, October 1989.

[6] Newell, A.C.; Francis, M.H.; Kremer, D.P., "The determination of near-field correction parameters for circularly polarized probes," Proceedings of the Antenna Measurement Techniques Association, vol. 6, pp. 3A3-1 to 3A3-29, October 1984.

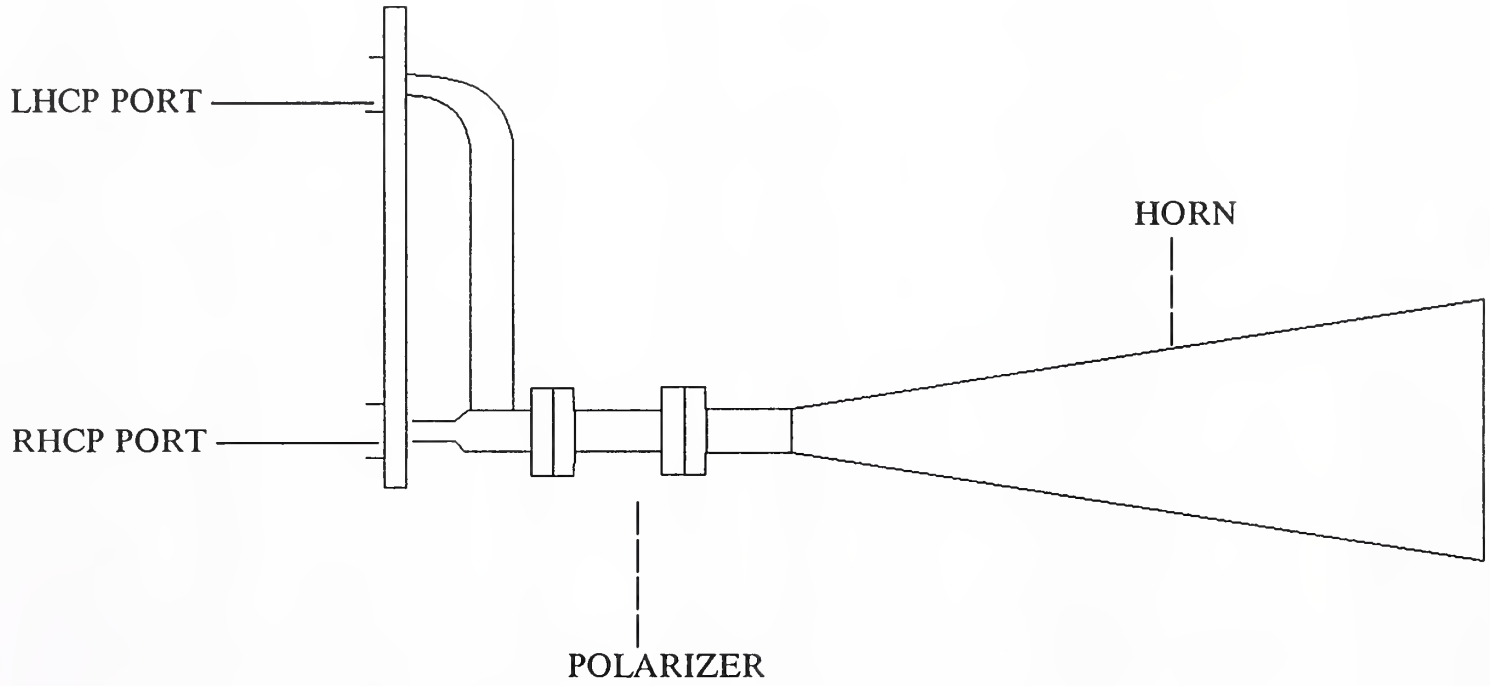

Figure 1. Typical probe assembly drawing.

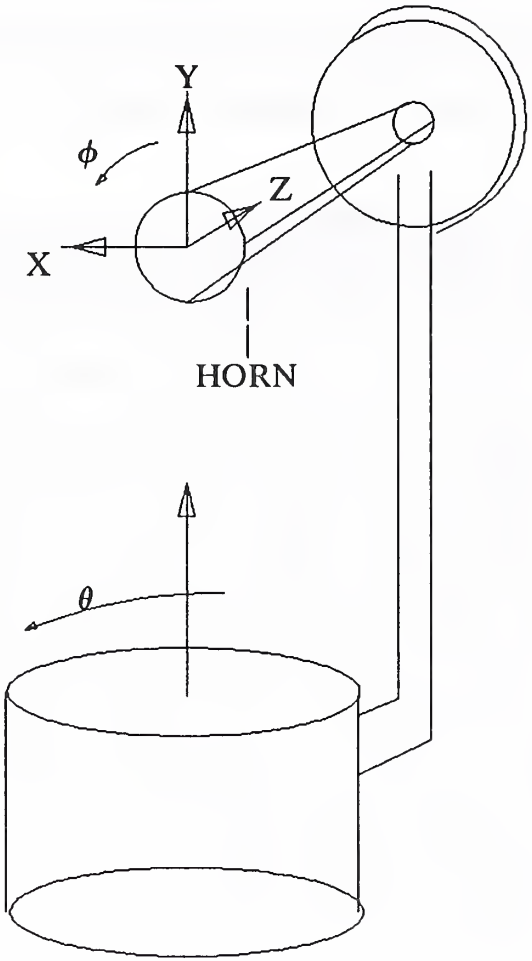

Figure 2. Illustration showing the axes of rotation for pattern measurements.

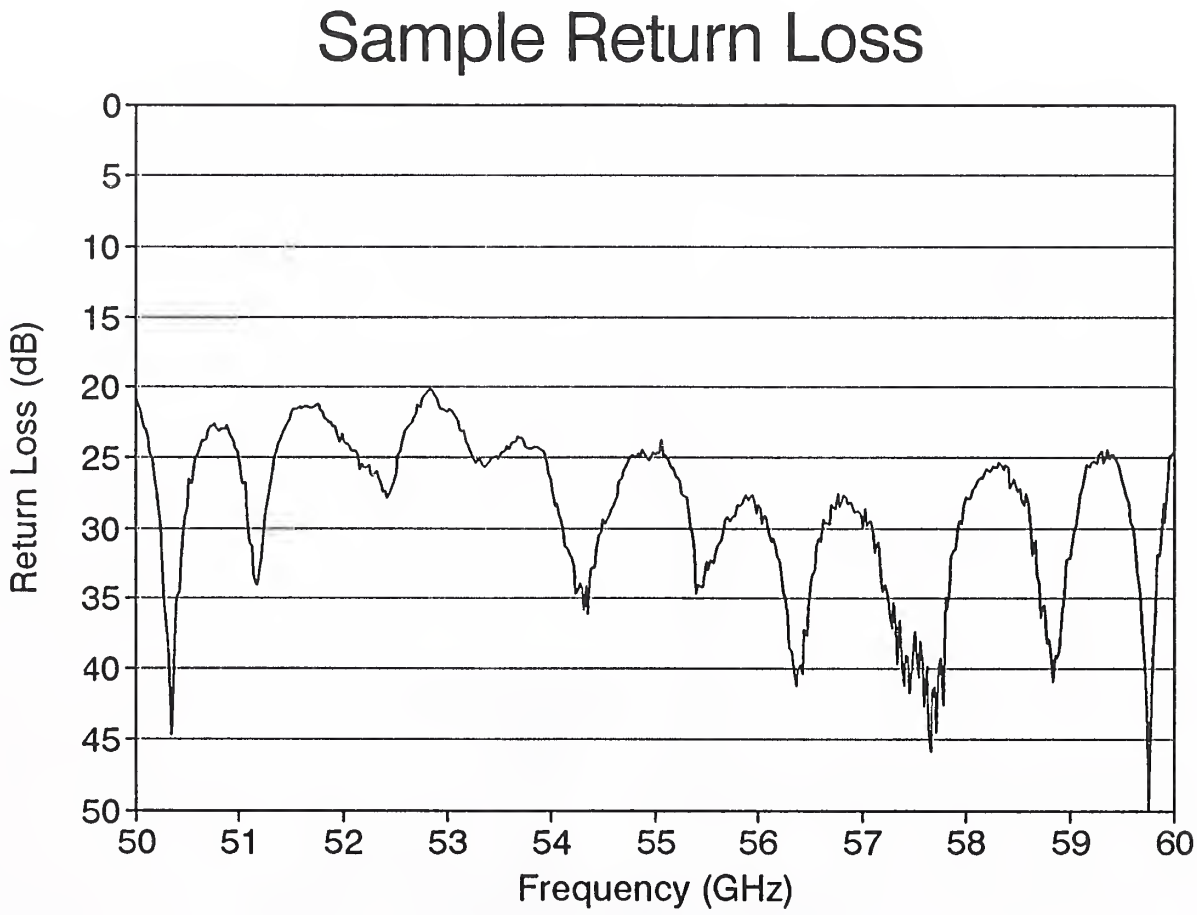

Figure 3. Sample return loss measurement.

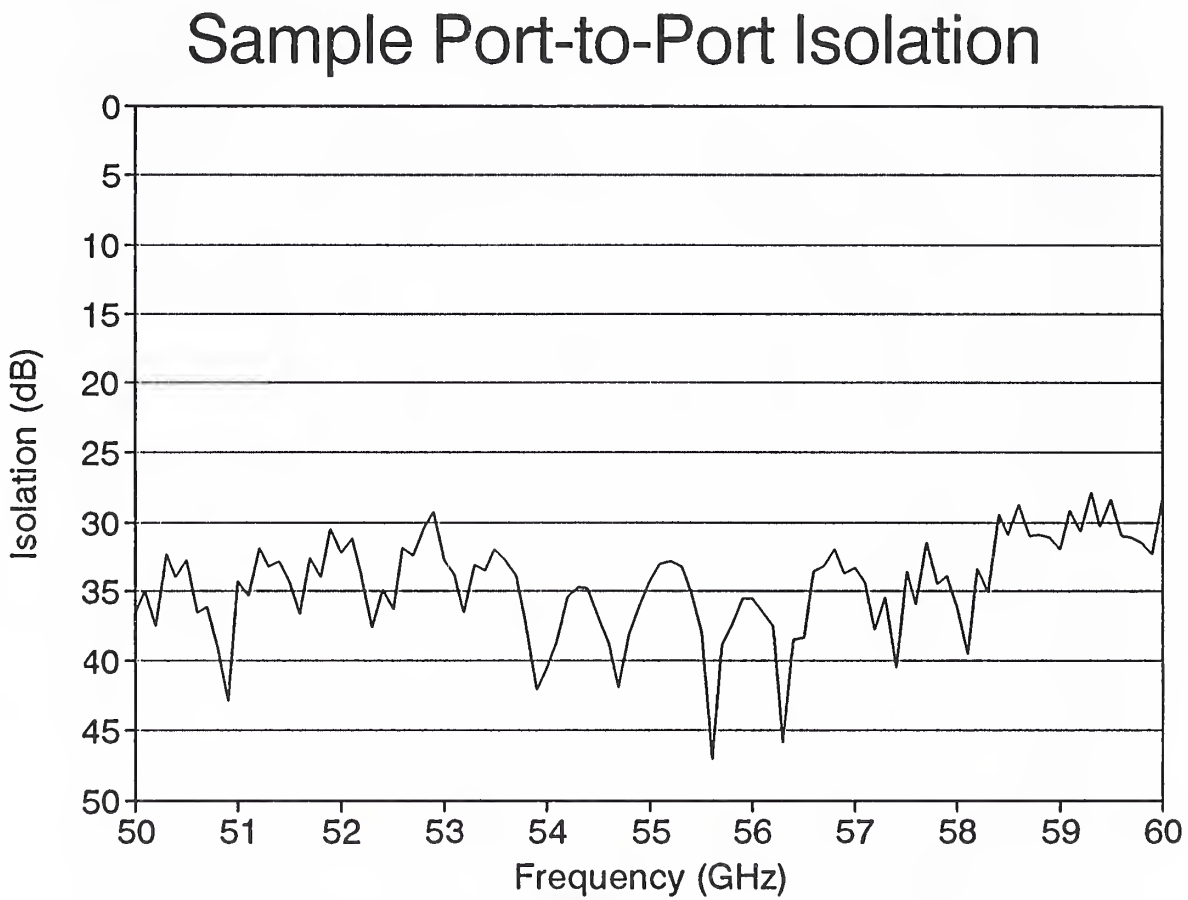

Figure 4. Sample port-to-port isolation measurement.

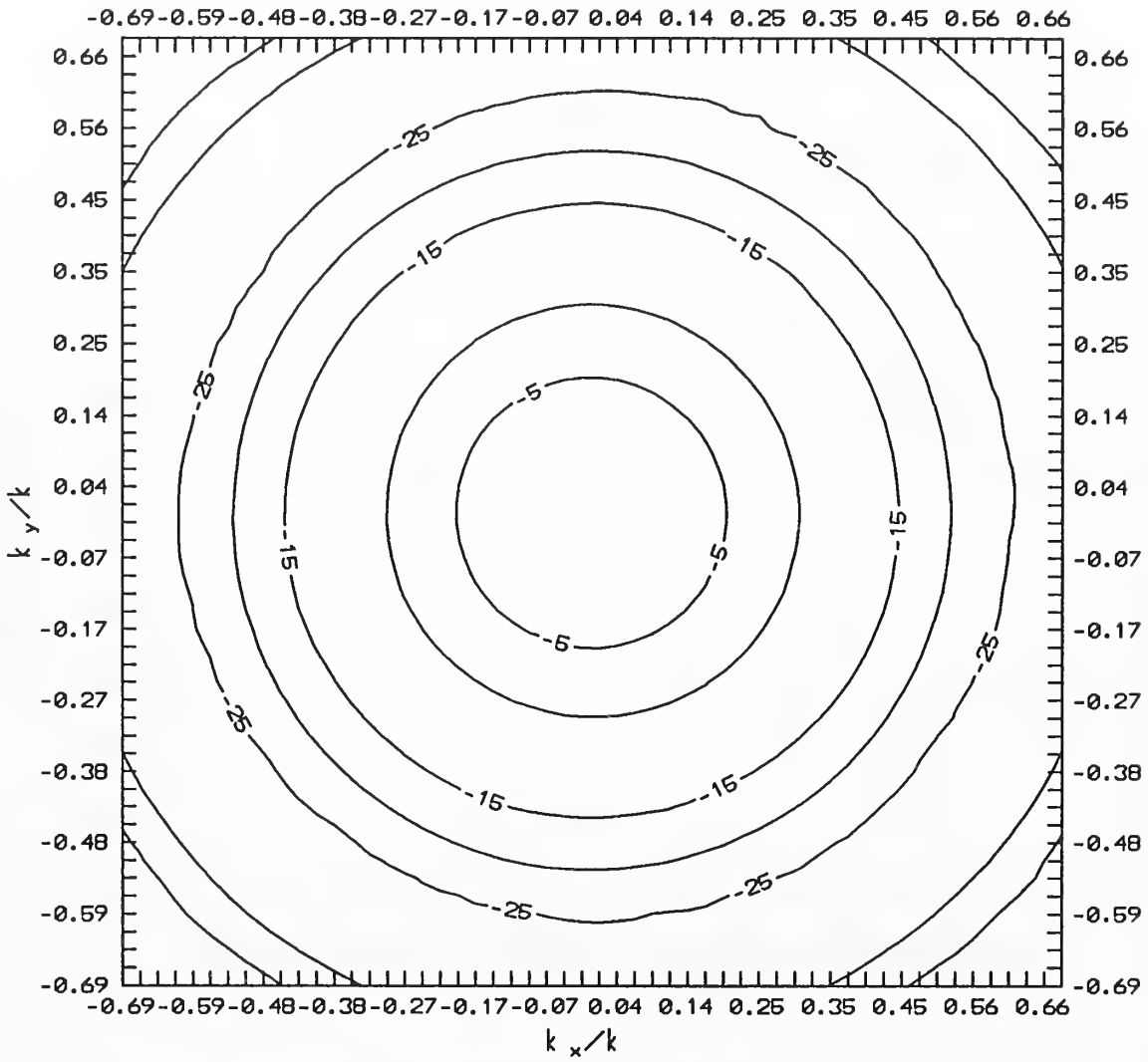

Figure 5. Sample main-component amplitude pattern, 5 dB contours.

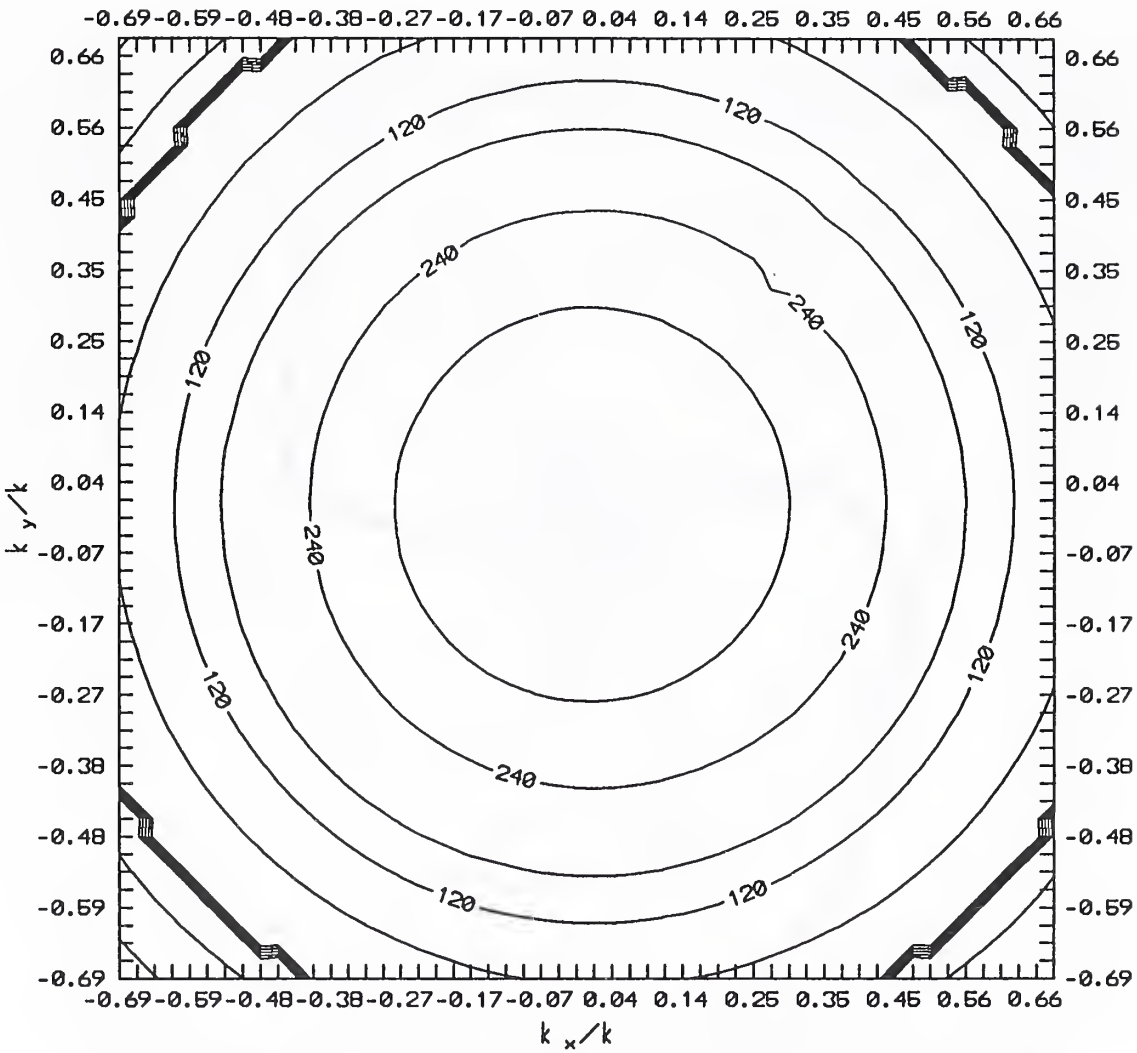

Figure 6. Sample main-component phase pattern, 60 degree contours.

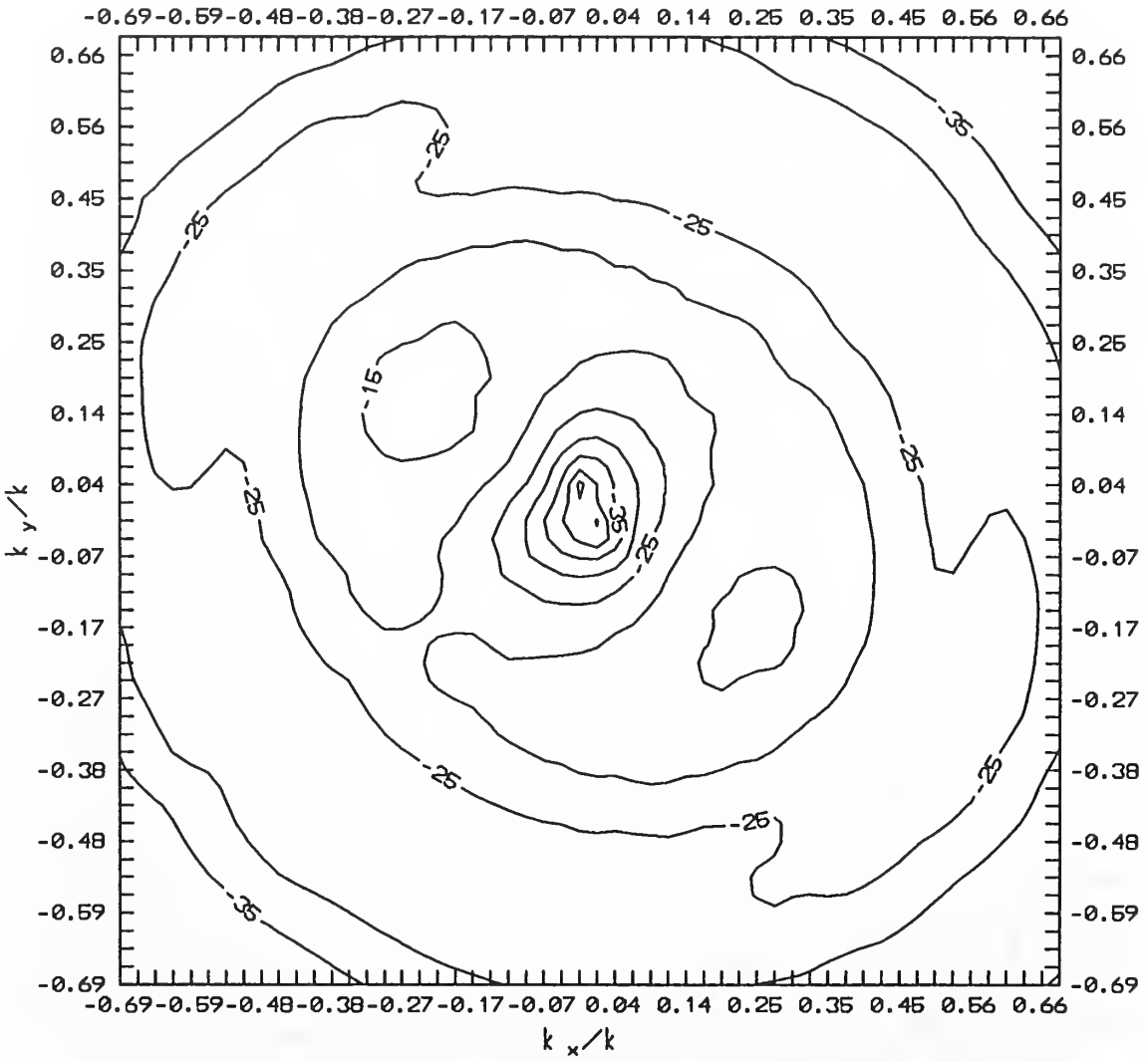

Figure 7. Sample cross-component amplitude pattern, 5 dB contours.

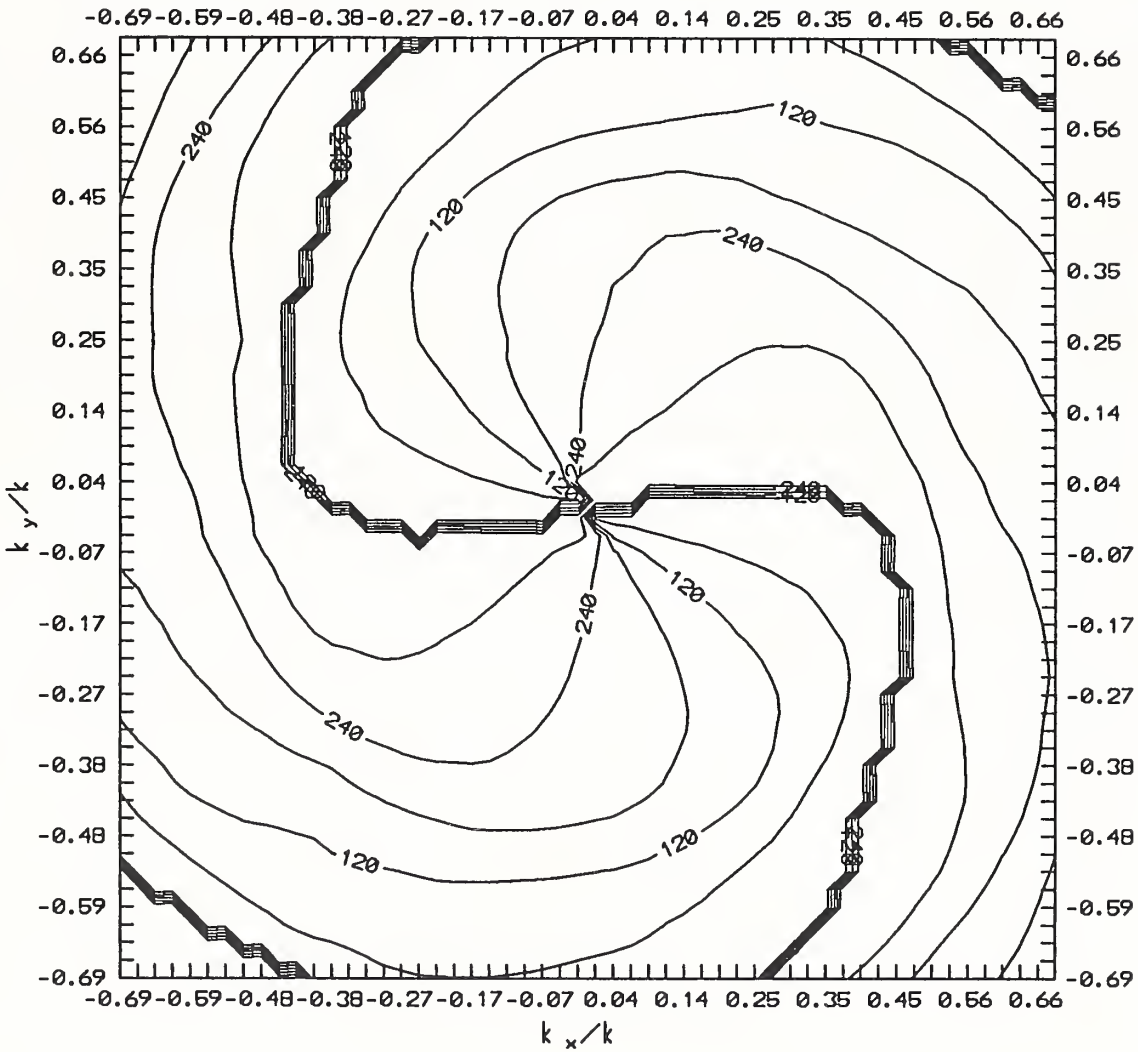

Figure 8. Sample cross-component phase pattern, 60 degree contours.